

Spectroscopy of Electronic States in InSb Quantum Dots

Ch. Sikorski and U. Merkt

Institut für Angewandte Physik, Universität Hamburg, D-2000 Hamburg 36, West Germany

(Received 22 December 1988)

We have realized arrays of quantum dots on InSb and observe intraband transitions between their discrete (zero-dimensional) electronic states with far-infrared magnetospectroscopy. In our devices, the number of electrons can be adjusted by a gate voltage and less than five electrons per dot are detectable.

PACS numbers: 73.20.Dx, 72.15.Rn, 78.30.Fs

Progress of nanofabrication technology now renders it possible to laterally confine electrons on semiconductors to quantum wires and quantum dots.¹ Both systems take advantage of quasi-two-dimensional (2D) electron gases present in heterostructures, quantum wells, or metal-oxide-semiconductor devices.² Quantum wires are obtained by confinement in one of the two directions in the plane of the 2D gas. Consequently, the electrons can move freely only along the remaining direction and thus constitute a 1D gas of a quantum wire. Confinement in both directions results in a 0D gas of a quantum dot.

Zero-dimensional electronic behavior recently has been demonstrated unambiguously by resonant tunneling³ through laterally constricted InGaAs quantum wells and by capacitance oscillations⁴ of microstructured GaAs/GaAlAs heterojunctions. Here, we report the direct observation of resonance transitions between discrete states of quantum dots on InSb. The particular advantage of this narrow-gap semiconductor is its small effective electron mass $m^* = 0.014m_e$ at the conduction-band edge. It gives rise to comparatively high quantization energies ≈ 10 meV for electronically active widths of typically 100 nm which can be achieved laterally with present semiconductor technology.^{5,6}

The application of a magnetic field to quantum dots offers interesting possibilities to study few-electron systems. Since the cyclotron energy $\hbar\omega_c$ readily can be made much larger than the binding energy of the confining electric potential, we can examine the transition from electrically bound states to Landau-type magnetic levels in this system. In real atoms, observation of transitions between magnetic-type levels, e.g., quasi-Landau resonances, only is feasible when the electrons are excited to high Rydberg states⁷ or when the atoms are exposed to megatesla fields⁸ present near pulsars. More closely, our system is related to the one of shallow donors in semiconductors.⁹ In contrast to donor atoms, however, we can adjust not only the size of our dots but also their electron number.

Arrays of $\approx 10^8$ dots are prepared on *p*-type InSb (111) surfaces of typical areas 3×3 mm². Samples covered with photoresist are exposed twice in a holographic setup which employs an argon laser ($\lambda = 458$ nm) whose expanded beam is split into two partial

beams. The partial beams interfere near the sample and thus create a periodic intensity pattern of grating constant $a = 250$ nm in the photoresist. After the first exposure, the sample is rotated by an angle of 90° and exposure is repeated. Subsequent to development the samples are etched in an oxygen plasma. This removes resist residues between the dots and reduces the dot heights to values below 50 nm. We then evaporate a NiCr film which acts as a Schottky depletion gate⁵ at the NiCr/InSb interface between the dots; i.e., there we pin the Fermi energy E_F within the InSb band gap. A monitor sample metallized with Au is shown in Fig. 1 together with a schematic sketch of the band structure across the

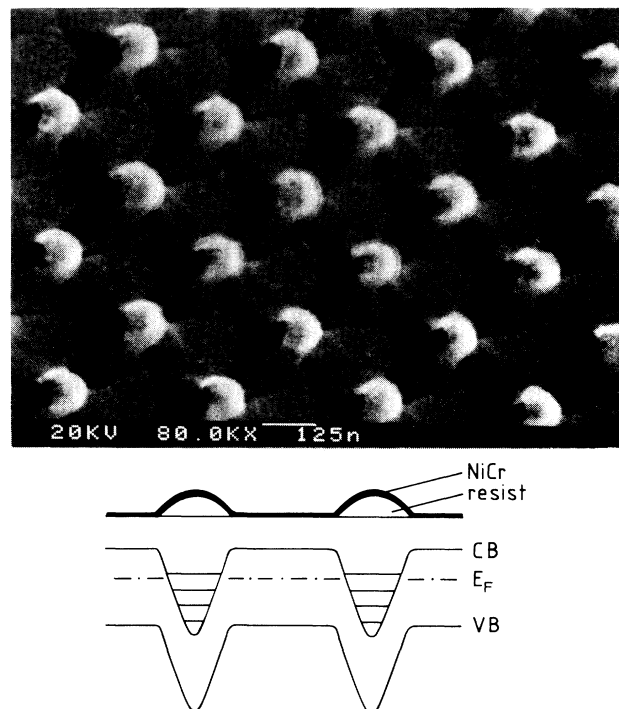


FIG. 1. Scanning electron micrograph of resist dots, with a 125 nm marker, together with a schematic sketch of the band structure across the dots right at the InSb surface. The bright disks give an idea of the geometrical dot size. This monitor sample is shadowed with gold for contrast enhancement.

dots. After deposition of ≈ 400 nm SiO_2 , we evaporate a second NiCr film as a gate contact. When a gate voltage V_g is applied between this contact and the InSb substrate, the number of mobile inversion electrons under the resist dots can be controlled by the field effect due to the finite resistivity ($R \approx 1 \text{ M}\Omega$) of the InSb substrate. The device becomes completely depleted of mobile electrons at the threshold voltage $V_t = -98 \text{ V}$.

Spectroscopy is carried out with an optically pumped far-infrared laser at liquid-helium temperature. The light impinges perpendicularly onto the sample and, hence, is polarized parallel to the surface. The relative change of transmittance $t = -[T(V_g) - T(V_t)]/T(V_t)$ is recorded versus the strength B of a magnetic field applied perpendicular to the surface. Spectra for various laser energies $\hbar\omega$ and gate voltages $\Delta V_g = V_g - V_t$ are shown in Fig. 2 for linearly polarized light. However, the spectra are almost independent of the polarization direction in the plane as is expected by virtue of sample preparation.

Spectra for the energy $\hbar\omega = 10.4 \text{ meV}$ resemble cyclotron resonances of a homogeneous 2D inversion layer but the resonance magnetic fields are already shifted considerably ($\Delta B \approx 0.4 \text{ T}$) to lower field strengths.¹⁰ This directly reflects the additional spatial quantization in the

confining lateral potential. For energy $\hbar\omega = 7.6 \text{ meV}$, we no longer observe a distinct resonance maximum at finite fields but a monotonic decrease of the relative transmittance when the magnetic field is increased. We will show below that this is indeed expected when the characteristic quantization energy of the lateral potential approximately coincides with the laser energy. For the energy $\hbar\omega = 3.2 \text{ meV}$, we again observe distinct but weak resonances at $B \approx 1.5 \text{ T}$. As we show next, these resonances are characteristic of a system which is confined in both lateral dimensions.

To obtain a simple description of electrons in quantum dots, we consider the harmonic-oscillator potential $\frac{1}{2} m^* \times \omega_0^2 (x^2 + y^2)$ with eigenfrequency ω_0 in a magnetic field directed along the z direction.¹¹ This parabolic model is expected to be a good approximation for low-electron numbers.¹² The single-electron eigenenergies of the lateral motion,

$$E_{nm} = (2n + |m| + 1) \hbar [(\omega_c/2)^2 + \omega_0^2]^{1/2} + (\hbar \omega_c/2) m, \quad (1)$$

depend on the radial $n=0,1,\dots$ and azimuthal $m=0, \pm 1, \dots$ quantum number. At low-electron numbers, only the lowest 2D subband is occupied.¹⁰ Figure 3 depicts the lowest energies versus magnetic field strength and the allowed dipole transitions which have resonance frequencies

$$\omega_{\pm} = [(\omega_c/2)^2 + \omega_0^2]^{1/2} \pm \omega_c/2, \quad (2)$$

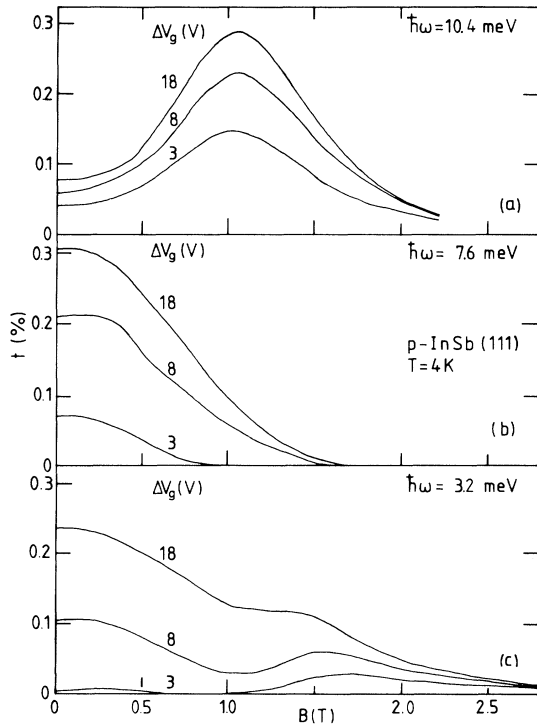


FIG. 2. Far-infrared spectra for three laser frequencies ω and three gate voltages ΔV_g . (a) ω_+ resonances at $B \approx 1.0 \text{ T}$ for a laser frequency above the quantization frequency ω_0 , (b) traces for $\omega = \omega_0$, and (c) ω_- resonances for $B \approx 1.5 \text{ T}$ for $\omega < \omega_0$.

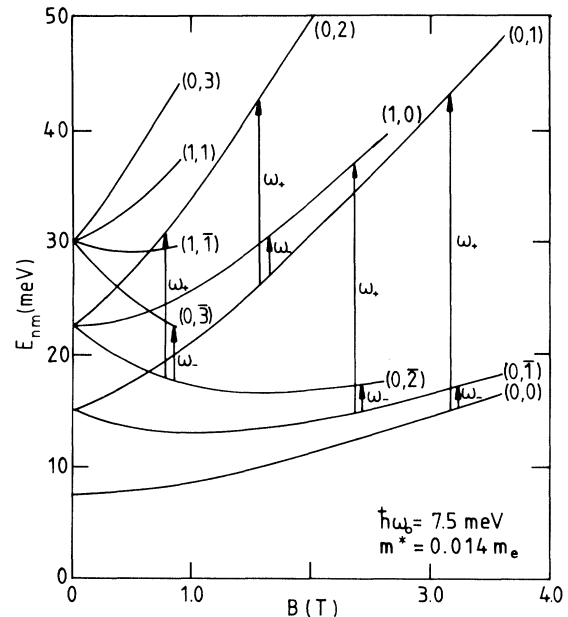


FIG. 3. Calculated level diagram of the oscillator potential $\frac{1}{2} m^* \omega_0^2 (x^2 + y^2)$ in a magnetic field $B \parallel z$. Levels are indicated by their quantum numbers (n, m) with $\bar{m} = -m$. For some initial states, transitions ω_{\pm} allowed for two circular light polarizations, respectively, are marked by arrows.

and which are excited with circular light polarizations \pm , respectively. At $B=0$ we have oscillator levels $(n'+1)\hbar\omega_0$, with the abbreviation $n'=2n+|m|$. In high magnetic fields ($\omega_c \gg \omega_0$), all levels with quantum numbers $n=0, m \leq 0$ converge and form a highly degenerate ground state of energy $\frac{1}{2}\hbar\omega_c$. Levels $n=1, m \leq 0$ converge to a common excited state $\frac{3}{2}\hbar\omega$. States with angular momentum $m > 0$ have much higher energies and do not contribute to the signals since they are no longer occupied. In this high magnetic field limit, transitions ω_+ become cyclotron resonances between Landau levels $\hbar\omega_c(n+\frac{1}{2})$ and the electron gas exhibits 2D behavior. Simultaneously, the oscillator strength of transitions ω_- vanishes. Therefore, these resonances are not observed in strong magnetic fields. To be more specific, they are characteristic of a confined system with a radius comparable to or less than the cyclotron radius $l=(\hbar/eB)^{1/2}$.

To model our line shapes, we first calculate classical conductivities

$$\sigma_{\pm}(\omega) = \frac{en_0\mu}{1 + [(\omega_0^2/\omega) - \omega \pm \omega_c]^2 \tau^2} \quad (3)$$

for circular light polarizations from the classical equation of motion with a phenomenological relaxation time τ and a mobility $\mu = e\tau/m^*$. We then take into account the quantum-mechanical oscillator strengths.¹¹ The relation between conductivity and relative change of transmittance

$$t \cong \frac{1}{a^2} \frac{2\sigma(\omega)/Y_0}{1 + \sqrt{\epsilon} + \sigma_{\square}/Y_0} \quad (4)$$

is adopted from its 2D counterpart¹³ with InSb dielectric constant $\epsilon=17$, wave admittance $Y_0=(377 \Omega)^{-1}$, and effective sheet conductivity $\sigma_{\square}=(18 \Omega)^{-1}$ of the two NiCr films. The conductivity $\sigma \cong (\omega_+ \sigma_+ + \omega_- \sigma_-)/(\omega_+ + \omega_-)$ for linearly polarized light incorporates the oscillator strengths and proves to be nearly independent of level occupation. Equation (4) qualitatively describes the observed line shapes. In particular, it explains cyclotronlike ω_+ resonances at frequencies $\omega > \omega_0$, monotonic intensity decreases proportional to $(1 + \mu^2 B^2)^{-1}$ at $\omega \cong \omega_0$, and weak intensities of ω_- resonances at $\omega < \omega_0$.

Most important, it allows us to determine the average number n_0 of electrons in a dot. This is most readily

TABLE I. Average electron number n_0 per dot, quantum number n' of the highest populated ($B=0$) oscillator level, and electronically active dot radius r_F . Values are given for three gate voltages $\Delta V_g = V_g - V_1$.

ΔV_g (V)	n_0	n'	r_F (nm)
3	3 ± 1	1	54
8	9 ± 1	2	66
18	20 ± 2	3	76

done with spectra taken at frequencies $\omega \cong \omega_0$ where we have the relation $t(B=0) \cong 2en_0\mu/\sigma_{\square}a^2$ for conductivities $\sigma_{\square} \gg Y_0$. Mobilities $\mu = (B_{1/2})^{-1} \cong 20000 \text{ cm}^2 \text{ V}^{-1} \text{ s}^{-1}$ are obtained from the fields $B_{1/2}$ where the transmittances have dropped to half of their maximum values at $B=0$. Electron numbers n_0 , quantum numbers $n'=2n+|m|$ of the highest populated $B=0$ level, and electronic dot radii $r_F = [2\hbar(n'+1)/m^*\omega_0]^{1/2}$ at the Fermi energies $E_F \cong 15, 22.5, \text{ and } 30 \text{ meV}$ are summarized in Table I for the gate voltages of Fig. 2. Almost the same electron numbers n_0 are obtained when cyclotronlike resonances for a much higher energy $\hbar\omega = 26.6 \text{ meV}$ are fitted with theoretical line shapes¹⁰ of 2D cyclotron resonance. Difference between numbers obtained for frequencies $\omega \cong \omega_0$ (lateral electric oscillator) and $\omega \gg \omega_0$ (Landau oscillator) are given as experimental uncertainties in Table I. For reasons we do not yet understand in detail, the number of electrons saturates at voltages above $\Delta V_g = 20 \text{ V}$.

Experimental resonance positions for gate voltage $\Delta V_g = 8 \text{ V}$ are given in Fig. 4 together with theoretical curves calculated from Eq. (2). At the highest energy ($\hbar\omega \cong \hbar\omega_c \gg \hbar\omega_0$) there is a shift $\Delta B = 0.8 \text{ T}$ between the experimental and theoretical results. This shift is almost quantitatively explained by the influence of band nonparabolicity¹⁴ which at the lower energies is less important. For lower energies, Eq. (2) provides a qualitative description and we can estimate the quantization energy $\hbar\omega_0 = 7.5 \pm 1 \text{ meV}$. This value agrees with the one which we already deduced from the shape of the $\hbar\omega = 7.6 \text{ meV}$ spectra in Fig. 2.

Within experimental error, the quantization energy does not depend on electron number in the range $n_0 = 3$ to 20. This provides strong evidence that collective depolarization modes which might be expected to become important at higher electron numbers^{15,16} are strongly suppressed in our devices. In fact, macroscopic electric fields are effectively screened by the NiCr Schottky gate since it is evaporated in very close vicinity to the electron

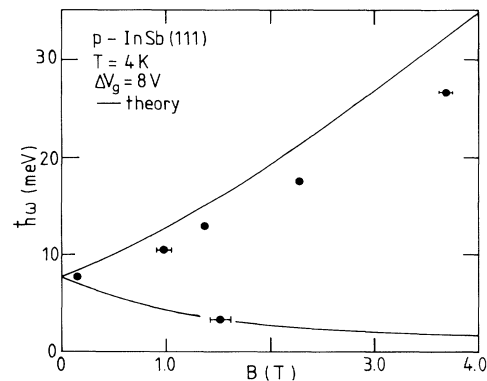


FIG. 4. Resonance positions for gate voltage $\Delta V_g = 8 \text{ V}$. The solid lines are calculated from Eq. (2) for parameters $\hbar\omega_0 = 7.5 \text{ meV}$ and $m^* = 0.014m_e$.

systems.⁶ For the same reason, we do not expect electromagnetic coupling between dots.

To conclude, we directly detect intraband transitions between discrete states of quantum dots on InSb. The number of electrons n_0 per dot can be controlled and switched by a gate voltage. We determine quantization energies of about 7 meV for zero magnetic fields and deduce electron numbers $n_0=3$ to 20. This means that we approach an ultimate limit set to the miniaturization of electronically active semiconductor devices, namely one electron per dot.

We thank J. P. Kotthaus for valuable discussions and acknowledge financial support of the Deutsche Forschungsgemeinschaft and the Stiftung Volkswagenwerk.

¹*Physics and Technology of Submicron Structures*, edited by H. Heinrich, G. Bauer, and F. Kuchar, Springer Series in Solid-State Sciences Vol. 83 (Springer-Verlag, Berlin, 1988).

²T. Ando, A. B. Fowler, and F. Stern, *Rev. Mod. Phys.* **54**, 437 (1982).

³M. A. Reed, J. N. Randall, R. J. Aggarwal, R. J. Matyi, T. M. Moore, and A. E. Wetsel, *Phys. Rev. Lett.* **60**, 535 (1988).

⁴T. P. Smith, III, K. Y. Lee, C. M. Knoedler, J. M. Hong,

and D. P. Kern, *Phys. Rev. B* **38**, 2172 (1988).

⁵W. Hansen, M. Horst, J. P. Kotthaus, U. Merkt, Ch. Sikorski, and K. Ploog, *Phys. Rev. Lett.* **58**, 2586 (1987).

⁶J. Alsmeyer, Ch. Sikorski, and U. Merkt, *Phys. Rev. B* **37**, 4314 (1988).

⁷J. Neukammer, H. Rinneberg, K. Vietzke, A. König, H. Hieronymus, M. Kohl, H. J. Grabka, and G. Wunner, *Phys. Rev. Lett.* **59**, 2947 (1987).

⁸H. Ruder, H. Herold, W. Rösner, and G. Wunner, *Physica (Amsterdam)* **127B**, 11 (1984).

⁹Y. Yafet, R. W. Keyes, and E. N. Adams, *J. Phys. Chem. Solids* **1**, 137 (1956).

¹⁰U. Merkt, M. Horst, T. Ebelbauer, and J. P. Kotthaus, *Phys. Rev. B* **34**, 7234 (1986).

¹¹R. B. Dingle, *Proc. Roy. Soc. London, Ser. A* **211**, 500 (1952); **212**, 38 (1952). This treatment of the Landau quantization in the symmetric gauge allows us to include the lateral oscillator potential in an easy way.

¹²S. E. Laux, D. J. Frank, and F. Stern, *Surf. Sci.* **196**, 101 (1988).

¹³S. J. Allen, Jr., D. C. Tsui, and F. DeRosa, *Phys. Rev. Lett.* **35**, 1359 (1975).

¹⁴U. Merkt and S. Oetling, *Phys. Rev. B* **35**, 2460 (1987).

¹⁵S. J. Allen, Jr., H. L. Störmer, and J. C. M. Hwang, *Phys. Rev. B* **28**, 4875 (1983).

¹⁶W. Que and G. Kirczenow, *Phys. Rev. B* **38**, 3614 (1988).

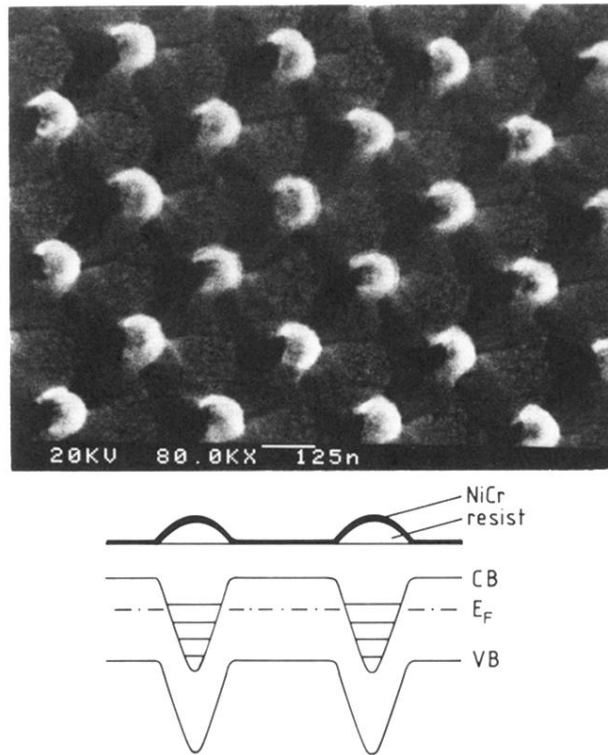


FIG. 1. Scanning electron micrograph of resist dots, with a 125 nm marker, together with a schematical sketch of the band structure across the dots right at the InSb surface. The bright disks give an idea of the geometrical dot size. This monitor sample is shadowed with gold for contrast enhancement.